

Synthesis and Characterization of $\text{Co}_x\text{O}_y/\text{MnCO}_3$ and $\text{Co}_x\text{O}_y/\text{Mn}_2\text{O}_3$ Catalysts: A Comparative Catalytic Assessment Towards the Aerial Oxidation of Various Kinds of Alcohols

Authors:

Osamah Alduhaish, Syed Farooq Adil, Mohamed E. Assal, Mohammed Rafi Shaik, Mufsiir Kuniyil, Khalid M. Manqari, Doumbia Sekou, Mujeeb Khan, Aslam Khan, Ahmed Z. Dewidar, Abdulrahman Al-Warthan, Mohammed Rafiq H. Siddiqui

Date Submitted: 2020-12-17

Keywords: oxygen, alcohols, oxidation, catalyst, manganese carbonate, cobalt oxide

Abstract:

$\text{Co}_x\text{O}_y/\text{manganese carbonate}$ ($X\%$)/($\text{Co}_x\text{O}_y/\text{MnCO}_3$ catalysts ($X = 1\text{?}7$)) were synthesized via a straightforward co-precipitation strategy followed by calcination at 300 °C. Upon calcination at 500 °C, these were transformed to $\text{Co}_x\text{O}_y/\text{manganese trioxide}$ i.e., ($X\%$)/ $\text{Co}_x\text{O}_y/\text{Mn}_2\text{O}_3$. A relative catalytic evaluation was conducted to compare the catalytic efficiency of the two prepared catalysts for aerial oxidation of benzyl alcohol (BzOH) to benzaldehyde (BzH) using O_2 molecule as a clean oxidant without utilizing any additives or alkalis. Amongst the different percentages of doping with Co_xO_y (0?7% wt./wt.) on MnCO_3 support, the (1%) $\text{Co}_x\text{O}_y/\text{MnCO}_3$ catalyst exhibited the highest catalytic activity. The influence of catalyst loading, calcination temperature, reaction time, and temperature and catalyst dosage was thoroughly assessed to find the optimum conditions of oxidation of benzyl alcohol (BzOH) for getting the highest catalytic efficiency. The (1%) $\text{Co}_x\text{O}_y/\text{MnCO}_3$ catalyst which calcined at 300 °C displayed the best effectiveness and possessed the largest specific surface area i.e., 108.4 m^2/g , which suggested that the calcination process and specific surface area play a vital role in this transformation. A 100% conversion of BzOH along with BzH selectivity >99% was achieved after just 20 min. Notably, the attained specific activity was found to be considerably larger than the previously-reported cobalt-containing catalysts for this transformation. The scope of this oxidation reaction was expanded to various alcohols containing aromatic, aliphatic, allylic, and heterocyclic alcohols without any further oxidation i.e., carboxylic acid formation. The scanning electron microscope (SEM), energy-dispersive X-ray spectroscopy (EDS), X-ray diffraction (XRD), fourier transform infrared spectroscopy (FTIR), thermogravimetric analysis (TGA), and Brunauer?Emmett?Teller (BET) specific surface area analytical techniques were used to characterize the prepared catalysts. The obtained catalyst could be easily regenerated and reused for six consecutive runs without substantial decline in its efficiency.

Record Type: Published Article

Submitted To: LAPSE (Living Archive for Process Systems Engineering)

Citation (overall record, always the latest version):

LAPSE:2020.1184

Citation (this specific file, latest version):

LAPSE:2020.1184-1

Citation (this specific file, this version):








LAPSE:2020.1184-1v1

DOI of Published Version: <https://doi.org/10.3390/pr8080910>

License: Creative Commons Attribution 4.0 International (CC BY 4.0)

Article

Synthesis and Characterization of $\text{Co}_x\text{O}_y\text{-MnCO}_3$ and $\text{Co}_x\text{O}_y\text{-Mn}_2\text{O}_3$ Catalysts: A Comparative Catalytic Assessment Towards the Aerial Oxidation of Various Kinds of Alcohols

Osamah Alduhaish ¹, Syed Farooq Adil ^{1,*}, Mohamed E. Assal ¹, Mohammed Rafi Shaik ¹, Mufsir Kuniyil ¹, Khalid M. Manqari ¹, Doumbia Sekou ¹, Mujeeb Khan ^{1,*}, Aslam Khan ², Ahmed Z. Dewidar ³, Abdulrahman Al-Warthan ¹ and Mohammed Rafiq H. Siddiqui ¹

¹ Department of Chemistry, College of Science, King Saud University, P.O. 2455, Riyadh 11451, Saudi Arabia; oalduhaish@ksu.edu.sa (O.A.); masl@ksu.edu.sa (M.E.A.); mrshaik@ksu.edu.sa (M.R.S.); mkuniyil@ksu.edu.sa (M.K.); khlodraeh@gmail.com (K.M.M.); sdoumbia333@gmail.com (D.S.); awarthan@ksu.edu.sa (A.A.-W.); rafiqs@ksu.edu.sa (M.R.H.S.)

² King Abdullah Institute for Nanotechnology, King Saud University, Riyadh 11451, Saudi Arabia; aslamkhan@ksu.edu.sa

³ Agricultural Engineering Department, King Saud University, P.O. Box 2460, Riyadh 11451, Saudi Arabia; adewidar@ksu.edu.sa

* Correspondence: sfadil@ksu.edu.sa (S.F.A.); kmujeeb@ksu.edu.sa (M.K.)

Received: 24 June 2020; Accepted: 28 July 2020; Published: 1 August 2020



Abstract: Co_xO_y -manganese carbonate ($X\%$)($\text{Co}_x\text{O}_y\text{-MnCO}_3$ catalysts ($X = 1\text{--}7$)) were synthesized via a straightforward co-precipitation strategy followed by calcination at 300 °C. Upon calcination at 500 °C, these were transformed to Co_xO_y -dimanganese trioxide i.e., ($X\%$) $\text{Co}_x\text{O}_y\text{-Mn}_2\text{O}_3$. A relative catalytic evaluation was conducted to compare the catalytic efficiency of the two prepared catalysts for aerial oxidation of benzyl alcohol (BzOH) to benzaldehyde (BzH) using O_2 molecule as a clean oxidant without utilizing any additives or alkalis. Amongst the different percentages of doping with Co_xO_y (0–7% wt./wt.) on MnCO_3 support, the (1%) $\text{Co}_x\text{O}_y\text{-MnCO}_3$ catalyst exhibited the highest catalytic activity. The influence of catalyst loading, calcination temperature, reaction time, and temperature and catalyst dosage was thoroughly assessed to find the optimum conditions of oxidation of benzyl alcohol (BzOH) for getting the highest catalytic efficiency. The (1%) $\text{Co}_x\text{O}_y\text{-MnCO}_3$ catalyst which calcined at 300 °C displayed the best effectiveness and possessed the largest specific surface area i.e., 108.4 m^2/g , which suggested that the calcination process and specific surface area play a vital role in this transformation. A 100% conversion of BzOH along with BzH selectivity >99% was achieved after just 20 min. Notably, the attained specific activity was found to be considerably larger than the previously-reported cobalt-containing catalysts for this transformation. The scope of this oxidation reaction was expanded to various alcohols containing aromatic, aliphatic, allylic, and heterocyclic alcohols without any further oxidation i.e., carboxylic acid formation. The scanning electron microscope (SEM), energy-dispersive X-ray spectroscopy (EDS), X-ray diffraction (XRD), fourier transform infrared spectroscopy (FTIR), thermogravimetric analysis (TGA), and Brunauer–Emmett–Teller (BET) specific surface area analytical techniques were used to characterize the prepared catalysts. The obtained catalyst could be easily regenerated and reused for six consecutive runs without substantial decline in its efficiency.

Keywords: cobalt oxide; manganese carbonate; catalyst; oxidation; alcohols; oxygen

1. Introduction

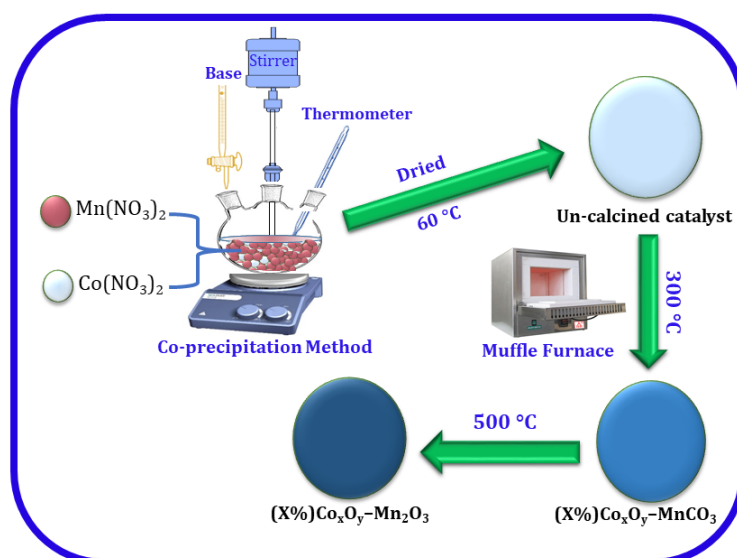
Catalytic oxidation of compounds, especially oxidation of organic alcohols to respective carbonyls, has extremely important organic synthetic transformation and industrial applications [1]. Carbonyls (e.g., aldehydes and ketones) are extensively applied as high value raw materials in pharmacology, perfumery, plastic additives, biofuels, confectionery, odorants, cosmetics, pesticides, flame-retardants, dyestuffs, and agrochemical industries [2]. This transformation is conventionally performed employing stoichiometric quantities of NaClO, CrO₃, SeO₂, RuO₄, Br₂, and Cr₂O₇, which are relatively costly, highly toxic, and corrosive in nature [3]. These protocols are environmentally unfavorable owing to the formation of copious amounts of hazardous wastes.

In recent years, significant efforts have been devoted to develop more environmentally-friendly methodologies to minimize the drawbacks of traditional oxidation approaches, including the substitution of costly, corrosive, and hazardous oxidants and the replacement of these with clean and inexpensive oxidants like hydrogen peroxide and molecular O₂ [4]. In particular, molecular O₂ has been widely employed for the catalytic oxidation of alcohol. This possesses several merits including the abundance of oxygen and its inexpensive and eco-friendly nature, in addition to the formation of water as the only by-product [5]. In this context, there has been considerable interest in the enhancement of efficient catalytic strategies based on noble metals, like Pd [6], Pt [7], Au [8], Rh [9], and Ru [10], some of which possess high activity for this chemical transformation. The expensive cost, difficulty in preparation, and scarcity of these precious metals have restricted the commercialization of these catalysts [11]. Consequently, massive efforts have made to substitute these costly metals with cheaper, earth-abundant transition metals, such as Cu [12], Ni [13], Fe [14], V [15], Cr [16], Mo [17], Zr [18], and Zn [19] for this oxidation process.

In addition, it is well known that the catalytic efficiency of metal or metal oxide nanoparticle (NP)-based catalysts improves noticeably after doping these catalysts with other metals, which could be ascribed to huge specific surface area of metallic NPs [20]. Moreover, manganese-based catalysts have been broadly utilized for oxidation of moieties such as CO [21], naphthalene [22], toluene [23], cyclohexane [24], alkynes [25], alkyl aromatics [26], and aldehydes [27]. In particular, manganese oxides containing catalysts have also been widely used in catalytic alcohol oxidation to respective aldehydes or ketones [28].

Apart from Mn catalysts, Co₃O₄ NPs have been assessed in catalytic oxidation of BzOH and showed higher catalytic activity towards oxidation of alcohols [29]. Zhu et al. have efficiently synthesized Co₃O₄ NPs supported on activated carbon [30]. These NPs exhibited about 100% conversion of BzOH as well as 87% selectivity towards BzH at 80 °C, as well as the catalyst showing no notable activity loss even after four recycling reactions. Additionally, Taghavimoghaddam et al. [31] synthesized mesoporous silica SBA-15-doped Co₃O₄, using impregnation and adsorption methods, which exhibited 31% alcohol conversion and 73% BzH selectivity.

In continuance of our present interest on the employment of several mixed metallic oxide NPs as highly effective catalysts for aerial oxidation of alcohols using O₂ molecule as an environmentally-benign oxidant without utilizing any co-oxidant or bases [32–34], we have reported the preparation of (X%)Co_xO_y–MnCO₃ (X = 0, 1, 3, 5, and 7) and thereafter calcination at 500 °C to synthesize (X%)Co_xO_y–Mn₂O₃. The as-obtained catalysts were evaluated for oxidation of a variety of alcohols to their respective carbonyls. The catalysts were synthesized via the co-precipitation procedure by changing the weight percentages of cobalt nitrate and manganese nitrate as illustrated in Scheme 1. Furthermore, the as-synthesized materials were thoroughly characterized via XRD, SEM, EDX, BET, TGA, and FTIR, to elucidate the oxidation mechanism. The catalytic behaviors of the prepared catalysts were thoroughly examined for oxidation of various kinds of alcohols.



Scheme 1. A pictorial illustration for the fabrication of $(X\%)Co_xO_y-MnCO_3$ calcined at $300\text{ }^\circ\text{C}$ and $(X\%)Co_xO_y-Mn_2O_3$ at $500\text{ }^\circ\text{C}$.

2. Experimental

2.1. Catalyst Fabrication

The $(X\%)Co_xO_y-MnCO_3$ catalysts ($X\% = 0\text{ wt.}\% - 7\text{ wt.}\%$), followed by calcination at $500\text{ }^\circ\text{C}$ to synthesize $(X\%)Co_xO_y-Mn_2O_3$, were prepared via the co-precipitation technique where $X\%$ denotes wt./wt. %. Standard solutions of $Mn(NO_3)_2 \cdot 4H_2O$ and $Co(NO_3)_2$ in distilled water were prepared and stoichiometric amounts of both solutions were mixed in a round-bottom-flask. The reaction mixture was heated up to $100\text{ }^\circ\text{C}$ and stirred vigorously, then, 0.5 M solution of $NaHCO_3$ was added drop-wise until the reaction mixture reached to $pH = 9$. The solution continued to be stirred at $100\text{ }^\circ\text{C}$ for 3 h and thereafter was left on stirring over-night at room temperature (RT). The resultant solution was washed several times and filtered by centrifugation and the obtained sample was dried at $65\text{ }^\circ\text{C}$ overnight and calcined in a muffle furnace (Nabertherm, Lilienthal, Germany) at various temperatures. The initial product formed was usually metal carbonate salts, which on calcination at elevated temperatures decomposed to metal oxides. A pictorial representation has been displayed in Scheme 1.

2.2. Characterization Techniques

The synthesized materials were characterized using several instruments and all experimental details are mentioned in Supplementary Materials.

2.3. Catalytic Assessment

Liquid-phase oxidation of benzyl alcohol was conducted in a three-necked glass flask equipped with a magnetic stirrer, reflux condenser, and thermometer. In a typical experiment, a mixture of the benzyl alcohol (2 mmol), toluene (15 mL), and the catalyst (300 mg) was transferred in a three-necked round-bottomed flask (100 mL), the resulting mixture was then heated to desired temperature with vigorous stirring along with bubbling oxygen gas at a flow rate of 25 mL min^{-1} into the reaction mixture. After the reaction, the solid catalyst was filtered off by centrifugation and the liquid products analyzed by gas chromatography to determine the conversion and product selectivity by (GC, 7890A) (Agilent Technologies Inc. Santa Clara, CA, United States) equipped with a flame ionization detector (FID) and a 19019S-001 HP-PONA column.

2.4. Reutilizing Tests

The used catalyst was extracted to be recycled by simple centrifugation followed by washing several times with toluene. It was then dried at 98 °C for 4 h before using it in the next recycling run under the optimal catalytic conditions.

3. Results and Discussion

3.1. Characterizations

Crystallographic structure of obtained materials was determined using XRD analysis. Figure 1 illustrates XRD analyses of catalyst calcined at 300 °C i.e., (1%)Co_xO_y-MnCO₃, and 500 °C i.e., (1%)Co_xO_y-Mn₂O₃. The obtained diffraction patterns revealed that the prepared catalysts were crystalline in nature. XRD pattern of catalyst calcined at 300 °C exhibited the existence of rhodochrosite MnCO₃ (JCPDS file no. 00-001-0981) (space group R-3c (167)). Upon the calcination at elevated temperature at 500 °C, this transformed to bixbyite dimanganese trioxide (Mn₂O₃) (JCPDS file No. 00-002-0909). The diffraction peaks related to Co_xO_y could not be identified owing to its low percentage in the catalyst. The crystallite size of the prepared samples was calculated using Debye–Scherrer equations and it was found to be 31 nm and 25.11 nm for (1%)Co_xO_y-MnCO₃ and (1%)Co_xO_y-Mn₂O₃, respectively.

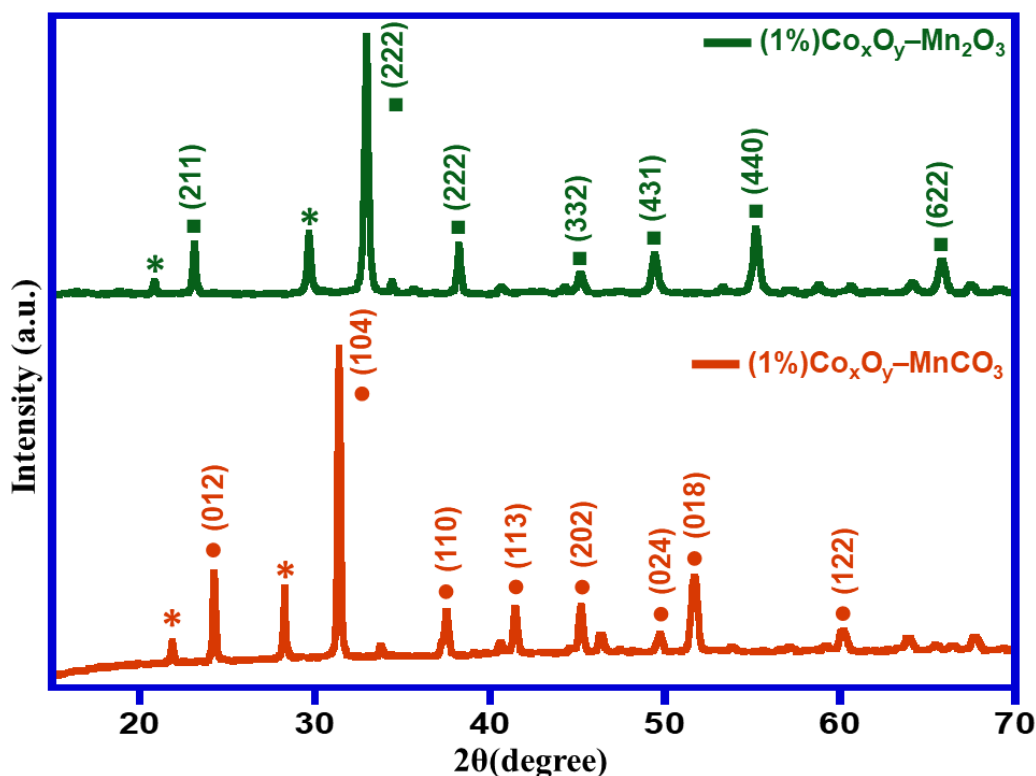


Figure 1. XRD diffractograms of the catalysts (1%)Co_xO_y-MnCO₃ calcined at 300 °C and (1%)Co_xO_y-Mn₂O₃ calcined at 500 °C. Denotations of the symbols are as follows: • MnCO₃, ■ Mn₂O₃, and * unidentified peaks.

The surface morphology of the as-obtained catalysts was identified using SEM analysis. The catalyst obtained using the co-precipitation procedure calcined at 300 °C (i.e., (1%)Co_xO_y-MnCO₃) and 500 °C (i.e., (1%)Co_xO_y-Mn₂O₃). The SEM images of the prepared catalysts (1%)Co_xO_y-MnCO₃ and (1%)Co_xO_y-Mn₂O₃ are represented in Figure 2. SEM images revealed that the morphology of as-synthesized catalysts possessed well-defined cuboidal morphology. Particle-size distributions of

the catalysts (1%)Co_xO_y-MnCO₃ and (1%)Co_xO_y-Mn₂O₃ were determined using Image J software program as demonstrated in Figure 2c,f. The particle-size distribution graphs displayed slight differences in the particle sizes with changes in calcination temperature. In addition, elemental composition of both catalysts, (1%)Co_xO_y-MnCO₃ and (1%)Co_xO_y-Mn₂O₃, were determined by EDS analysis, which revealed the elemental analysis summary of as-synthesized catalysts as demonstrated in Figure S1. Sharp signal at 5.894 keV strongly indicated the presence of 'Mn' as major element. Mn commonly has an optical absorption in this range owing to the surface plasmon resonance (SPR) phenomenon. A signal at 6.924 keV strongly indicated the existence of 'Co' element. It is also note-worthy that other signals found in the range of 0–0.5 keV, endorse typical absorption of C and O₂. Apparently, elemental compositions of catalysts are approximately identical to values of the composition anticipated while synthesizing the catalyst. Additionally, the samples were subjected to ICP analysis to confirm the exact composition of the catalyst and the percentage to Co_xO_y in the catalytic system was found to be 1.8%.

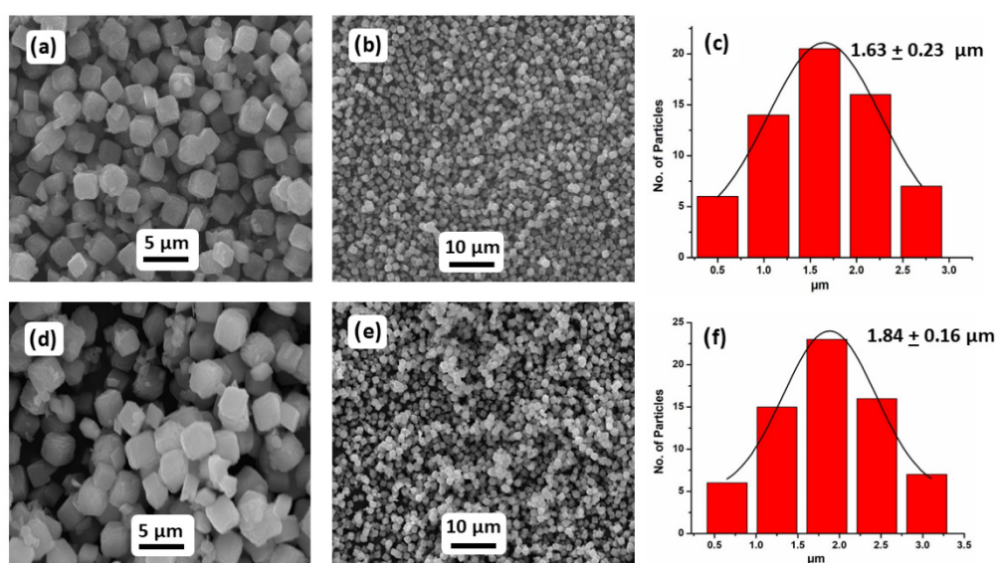


Figure 2. SEM analyses of prepared catalysts calcined at (a,b) 300 °C ((1%)Co_xO_y-MnCO₃) and (d,e) 500 °C ((1%)Co_xO_y-Mn₂O₃). (c) Particle-size distribution of (1%)Co_xO_y-MnCO₃ and (f) particle-size distribution of (1%)Co_xO_y-Mn₂O₃.

The surface functionalities of the prepared catalysts were studied using FTIR spectroscopy. FTIR analyses of catalysts at 300 °C and 500 °C calcination temperatures i.e., (1%)Co_xO_y-MnCO₃ and (1%)Co_xO_y-Mn₂O₃, respectively, are illustrated in Figure 3. High wavenumber area shows stretching vibrations of OH groups and absorbed H₂O molecules. The characteristic absorption spectral signals of ν-OH situated approximately at 3440 cm⁻¹ were found in 300 °C- and 500 °C-calcined catalysts, however a reduction in the intensities of these spectral signals was observed when the calcination temperature increased from 300 °C to 500 °C. This displays the decline of the existence of number of O-H groups on the catalyst surface. Furthermore, the spectral signals centered at ~1632 cm⁻¹ belong to bending modes of OH groups, which also displayed a decrease in intensity [35]. In the FTIR spectrum of (1%)Co_xO_y-MnCO₃ calcined at 300 °C, the existence of two absorption peaks located at around 858 and 1448 cm⁻¹ are reported as fingerprint peaks for MnCO₃, which was also confirmed by XRD and EDS results [36]. Additional, a peak at 1060 cm⁻¹, characteristic to vibrations of (C-O) bond, further confirmed the presence of the carbonate group in the catalyst calcined at 300 °C. For the 500 °C-calcined catalyst ((1%)Co_xO_y-Mn₂O₃), there were two bands at 858 and 1448 cm⁻¹ while the characteristic spectral signals for MnCO₃ were not found, revealing the total transformation of MnCO₃

to Mn_2O_3 at 500 °C calcination temperature. Intensive peaks were located in the range of 530–620 cm^{-1} that are fingerprint for several types of manganese oxides [37,38].

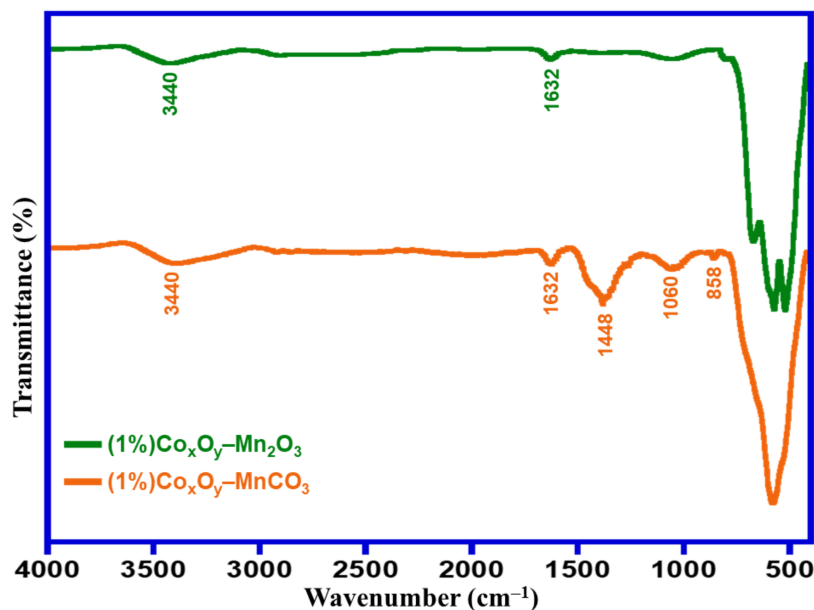


Figure 3. FTIR spectra of the catalysts calcined at 300 °C and 500 °C i.e., (1%) $\text{Co}_x\text{O}_y\text{-MnCO}_3$ and (1%) $\text{Co}_x\text{O}_y\text{-Mn}_2\text{O}_3$, respectively.

TGA analyses were conducted to assess the thermal stability of the as-prepared materials. This technique is especially advantageous for studying the thermal degradation of materials at various temperatures. The thermal stability of (1%) $\text{Co}_x\text{O}_y\text{-MnCO}_3$ calcined at 300 °C as well as (1%) $\text{Co}_x\text{O}_y\text{-Mn}_2\text{O}_3$ at 500 °C was evaluated by TGA as described in Figure 4. The thermogram of the catalyst calcined at 300 °C, i.e., (1%) $\text{Co}_x\text{O}_y\text{-MnCO}_3$, showed that it was stable up to 415 °C, with a slight weight loss of around 7% which could be ascribed to the exclusion of volatile impurities and adsorbed moisture. Raising the temperature led to an extra overall weight loss of 16% in the range of about 420–600 °C, which appears to be attributed to decarboxylation of MnCO_3 to produce MnO_2 and CO_2 , with the MnO_2 being oxidized to Mn_2O_3 , as reported by Zhu and co-workers [39].

To understand the variations in specific surface areas owing to the calcination process at various temperatures and the doping of the catalytic system with Co_xO_y , and to realize the linkage between the specific surface areas and catalytic activities of synthesized catalysts for this transformation, the specific surface area of prepared materials (i.e., (1%) $\text{Co}_x\text{O}_y\text{-MnCO}_3$, MnCO_3 , (1%) $\text{Co}_x\text{O}_y\text{-Mn}_2\text{O}_3$, and Mn_2O_3) was examined by BET analysis. Table 1 shows that specific surface area of the synthesized catalyst calcined at 300 °C and 500 °C i.e., (1%) $\text{Co}_x\text{O}_y\text{-MnCO}_3$ and (1%) $\text{Co}_x\text{O}_y\text{-Mn}_2\text{O}_3$, was approximately 108.4 and 56.7 m^2/g , respectively. From this it can be said that the specific surface area of the catalyst calcined at 300 °C i.e., (1%) $\text{Co}_x\text{O}_y\text{-MnCO}_3$, is larger than the catalyst obtained upon calcination at 500 °C i.e., (1%) $\text{Co}_x\text{O}_y\text{-Mn}_2\text{O}_3$. The attained data suggests that at higher calcination temperatures there is a decline in the specific surface area, presumably attributed to sintering. It is worth pointing out that sintering not only causes inter-particles, but it additionally diminishes the porosity in a single particle [40]. Notably, the uncalcined catalyst, i.e., (1%) $\text{Co}_x\text{O}_y\text{-MnCO}_3$, exhibited a surface area of 63.4 m^2/g , which confirms that the calcination temperature plays a fundamental role in enhancing the surface area of the catalytic system.

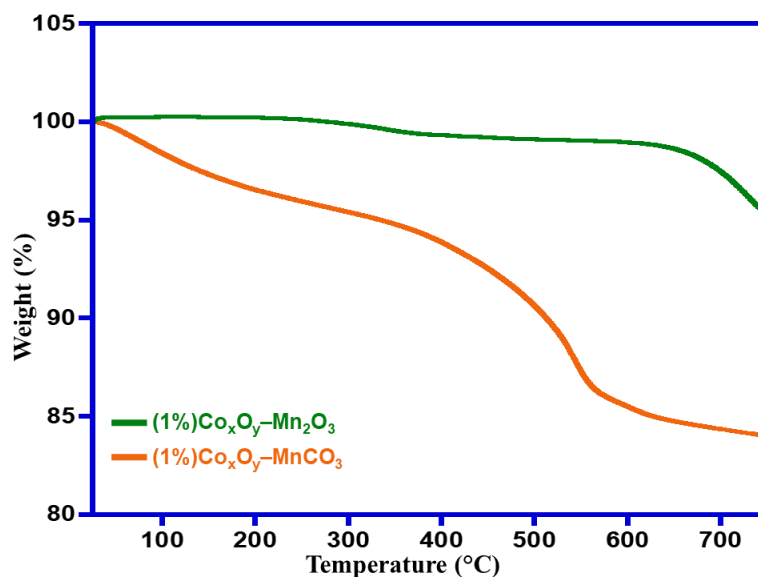


Figure 4. TGA curve of catalyst calcined at 300 °C and 500 °C i.e., (1%)Co_xO_y–MnCO₃ and (1%)Co_xO_y–Mn₂O₃, respectively.

Table 1. Calcination temperature optimization.

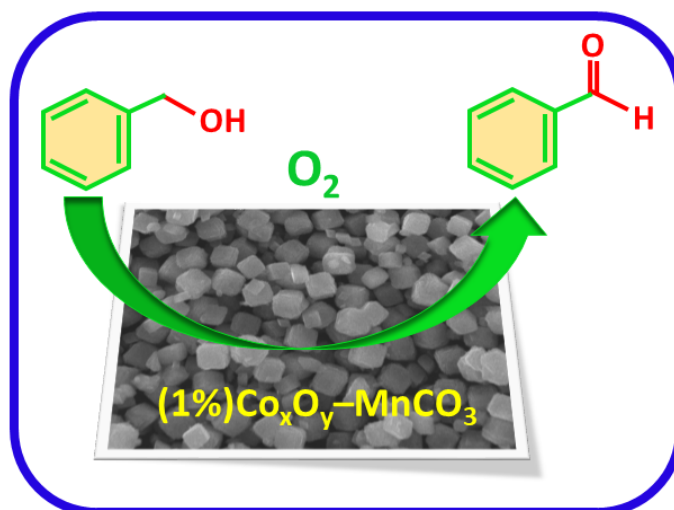
Entry	Catalyst	Calcination Temperature (°C)	Specific Surface Area (m ² /g)	Conversion (%)	Specific Activity (mmol/g·h)	Selectivity (%)
1	MnCO ₃	300	85.2	74.3	14.9	>99
2	Mn ₂ O ₃	500	24.1	49.3	9.9	>99
3	(1%)Co _x O _y –MnCO ₃	300	108.4	100.0	20.0	>99
4	(1%)Co _x O _y –Mn ₂ O ₃	500	56.7	65.8	13.2	>99

Conditions: 300 mg catalyst, 2 mmol BzOH, 15 mL toluene, 25 mL/min O₂ rate, 100 °C, 20 min.

Apart from the effect of calcination temperature, Co_xO_y has a promoting impact on catalytic efficiency by raising the specific surface area of manganese carbonate. The results show that after doping the catalyst with Co_xO_y, the specific surface area increased to 108.4 m²/g and yielded 100% conversion of BzOH, while the specific surface area of un-doped catalyst i.e., MnCO₃, was about 85.2 m²/g and gave 74.3% BzOH conversion. The substantial increase in the specific surface area after doping Co_xO_y might be responsible for enhancement of the catalytic performance, which can be attributed to existence of Co_xO_y on the MnCO₃'s surface. As a result, it can be stated that the synthesized catalyst upon calcination at different temperatures yields catalysts with different specific surface areas, which play a pivotal role in the efficiency of the synthesized catalyst. Hence from the above data, it can be deduced that the calcination temperature and the doping of Co_xO_y played a key role in varying the specific surface area of obtained catalysts, which in turn affected the catalytic performance.

3.2. Catalytic Performance Results

The oxidation of BzOH into BzH with gaseous O₂ as an eco-friendly oxidant acted as a template reaction to examine the activities of the as-synthesized catalysts (Scheme 2). To obtain the optimal conditions for best performance of the prepared catalysts, various parameters including catalyst loading, calcination temperature, reaction time, reaction temperature, and dosage of catalyst were thoroughly examined. To assess the influence of Co_xO_y, the catalytic performance of MnCO₃ and Mn₂O₃ was investigated under similar circumstances for comparison.



Scheme 2. Schematic depiction of oxidation of BzOH employing gaseous O_2 over the as-synthesized catalyst.

3.2.1. Influence of Calcination Temperature

As reported in previous literature, the calcination temperature has an explicit effect on the catalytic effectiveness of any heterogeneous catalyst [41]. The catalysts were calcined at 300 °C and 500 °C and the obtained materials examined for aerial oxidation of BzOH. The obtained data is presented in Figure 5 and listed in Table 1 and it can be seen that the catalytic conversion of BzOH to BzH is considerably affected by the calcination temperature of the catalyst. The catalyst calcined at 300 °C ($(1\%)Co_xO_y-MnCO_3$) afforded a 100% BzOH conversion with 20 mmol/g·h specific activity within only 20 min, while the catalyst calcined at 500 °C ($(1\%)Co_xO_y-Mn_2O_3$) exhibited a 65.8% conversion of BzOH with 13.2 mmol/g·h specific activity after 30 min under the identical catalytic circumstances (Entries 3 and 4). Notably, all catalysts exhibited excellent selectivity for BzH (>99%) (Entries 1–4). The presence of Co_xO_y on $MnCO_3$ and Mn_2O_3 played a fundamental role in enhancing the catalytic efficiency of synthesized catalysts, which could be ascribed to the synergistic interaction between Co_xO_y and Mn^{2+} [28]. However, the catalyst $(1\%)Co_xO_y-Mn_2O_3$ calcined at 500 °C exhibited lower catalytic efficiency as well as specific activity. This could probably be attributed to decomposition of the active sites of the catalyst or depreciation in specific surface areas, whilst the material calcined at 300 °C has manganese carbonate with active sites to promote catalysis. Moreover, from the spectral analysis it was observed that the $(1\%)Co_xO_y-MnCO_3$ catalyst possessed the O–H group on the catalyst surface, which was found to diminish (as per the intensity of the spectral signals) in the catalyst $(1\%)Co_xO_y-Mn_2O_3$, which was obtained upon calcination at 500 °C, indicating that the presence of the surface O–H group plays an essential part in this transformation [42]. Furthermore, the BET analysis shed light on the fact that the prepared catalyst i.e., $(1\%)Co_xO_y-MnCO_3$, calcined at 300 °C, had the highest specific surface area indicating that the specific surface area also plays an important role in the enhancement of catalytic performance. A similar trend was observed when the study was extended to compare the un-doped catalyst wherein the catalyst calcined at 300 °C i.e., $MnCO_3$, yielded a higher conversion product than that calcined at 500 °C i.e., Mn_2O_3 (Entries 1 and 2). Moreover, when the same reaction was carried out under identical conditions using the uncalcined, i.e., $(1\%)Co_xO_y-MnCO_3$, the conversion product obtained was found to be 13.38%, which is far lower than the 100% conversion product obtained by $(1\%)Co_xO_y-MnCO_3$ calcined at 300 °C. Hence, we chose to employ 300 °C as the optimal calcination temperature to improve other catalytic variables.

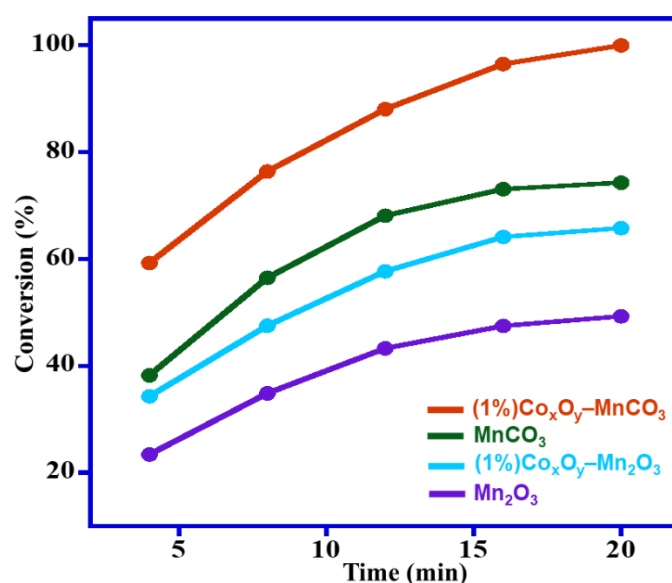


Figure 5. Graphical illustration of BzOH oxidation over catalysts calcined at 300 °C (i.e., (1%)Co_xO_y-MnCO₃ and MnCO₃) as well as the catalysts calcined at 500 °C (i.e., (1%)Co_xO_y-Mn₂O₃ and Mn₂O₃).

3.2.2. Influence of Weight % of Co_xO_y Promoter

The above results suggest that the catalyst calcined at 300 °C exhibited optimum catalytic activity, therefore further kinetic evaluations were performed using this calcination temperature. To further optimize the presence of Co_xO_y promoter, a series of catalysts were synthesized by altering weight % of Co_xO_y precursor from 0% to 7%. These were then examined for oxidation of BzOH to BzH and the attained data is compiled in Table 2. All catalysts were calcined at 300 °C, and the experiment was conducted at 100 °C. The catalyst with (1%)Co_xO_y as promoter i.e., (1%)Co_xO_y-MnCO₃, yielded a full conversion of BzOH alongside specific activity of 20 mmol/g·h (Entry 2). Furthermore, as the weight percentage of Co_xO_y was further increased, the catalysts (3%)Co_xO_y-MnCO₃, (5%)Co_xO_y-MnCO₃, and (7%)Co_xO_y-MnCO₃, exhibited lower alcohol conversions of 94.2%, 83.1%, and 65.4%, respectively (Entries 3–5). To confirm the existence of Co_xO_y as promoter, a catalyst synthesized without Co_xO_y i.e., MnCO₃, was subjected to identical catalytic process under similar circumstances. A 74.3% conversion of BzOH with 14.9 mmol/g·h specific activity was obtained, which shows the promotional impact of Co_xO_y in the catalytic system with 1 and 3 wt.% of Co_xO_y. The specific activity, was found to reduce with increased weight % of Co_xO_y from 1% to 3% in the catalyst. Moreover, a further increase in the weight % of Co_xO_y led to a further decline in the catalytic efficiency, which was probably due to blockage of active sites or to an aggregation of Co_xO_y on the surface of the catalyst. The graphical illustration is presented in Figure 6. From the above findings it is observed that, (1%)Co_xO_y-MnCO₃ catalyst is the best among the all catalysts prepared and hence it was selected for all the later studies designed to enhance further catalytic performance.

Table 2. Aerial oxidation of BzOH over the catalysts with varying % of Co_xO_y promoter.

Entry	Co _x O _y (%)	Catalyst	Conversion (%)	Specific Activity (mmol/g·h)	Selectivity (%)
1	0	(0%)Co _x O _y -MnCO ₃	74.3	14.9	>99
2	1	(1%)Co _x O _y -MnCO ₃	100.0	20.0	>99
3	3	(3%)Co _x O _y -MnCO ₃	94.2	18.8	>99
4	5	(5%)Co _x O _y -MnCO ₃	83.1	16.6	>99
5	7	(7%)Co _x O _y -MnCO ₃	65.4	13.1	>99

Conditions: 300 mg catalyst, 300 °C calcination temperature, 2 mmol BzOH, 15 mL toluene, 25 mL/min O₂ rate, 100 °C, 20 min.

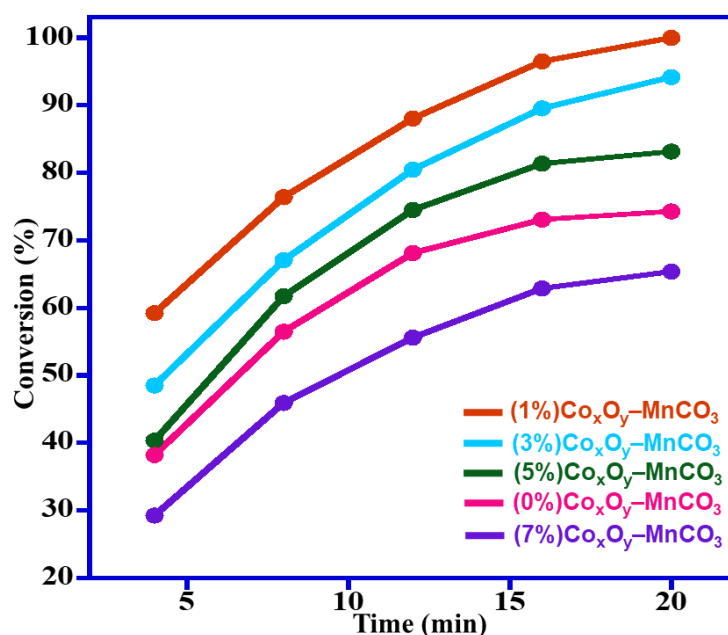


Figure 6. Graphical illustration of BzOH oxidation over (0%) $\text{Co}_x\text{O}_y\text{-MnCO}_3$, (1%) $\text{Co}_x\text{O}_y\text{-MnCO}_3$, (3%) $\text{Co}_x\text{O}_y\text{-MnCO}_3$, (5%) $\text{Co}_x\text{O}_y\text{-MnCO}_3$, and (7%) $\text{Co}_x\text{O}_y\text{-MnCO}_3$.

3.2.3. Influence of Temperature

It is well known that temperature plays a significant role in catalytic efficiency of a catalyst, which leads to enhanced oxidation rate. Therefore, the impact of temperature for the oxidation of BzOH is estimated by considering five temperatures ranging from room temperature (RT) to 100 °C using (1%) $\text{Co}_x\text{O}_y\text{-MnCO}_3$ catalyst, and while keeping other optimum parameters fixed. The obtained results are summarized in Table 3 and presented in Figure 7. The data presented in the Figure 7 reveals that the reaction temperature did influence the efficiency of the catalytic system, while, the selectivities toward BzH were found to be unaffected i.e., >99%. From the results obtained, it was found that at a lower temperature (RT), a relatively lower conversion of 35.7% was detected (Entry 1). Unsurprisingly, the higher temperature contributes to enhancement of the effectiveness of (1%) $\text{Co}_x\text{O}_y\text{-MnCO}_3$. At 100 °C, a complete transformation of BzOH and higher specific activity of 20 mmol/g·h, under the identical catalytic conditions was accomplished (Entry 5). Therefore, 100 °C was chosen to be an optimal temperature for reaction in all the further studies.

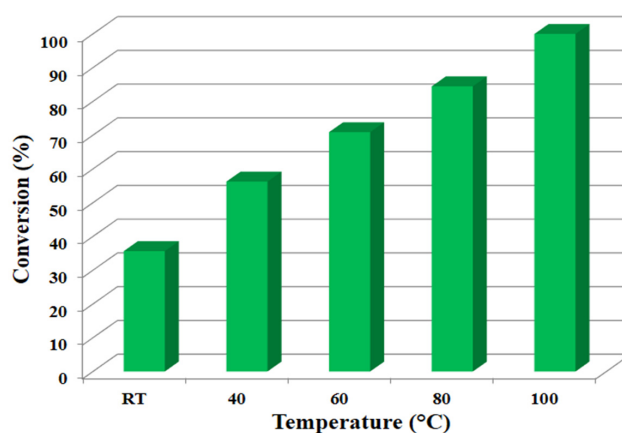


Figure 7. Dependence of conversion of BzOH on the reaction temperature catalyzed by (1%) $\text{Co}_x\text{O}_y\text{-MnCO}_3$.

Table 3. Reaction temperature optimization.

Entry	Temperature (°C)	Conversion (%)	Specific Activity (mmol/g·h)	Selectivity (%)
1	RT	35.7	7.1	>99
2	40	56.3	11.3	>99
3	60	70.9	14.2	>99
4	80	84.5	16.9	>99
5	100	100.0	20.0	>99

Conditions: 300 mg (1%)Co_xO_y-MnCO₃ catalyst, 300 °C calcination temperature, 2 mmol BzOH, 15 mL toluene, 25 mL/min O₂ rate, 20 min.

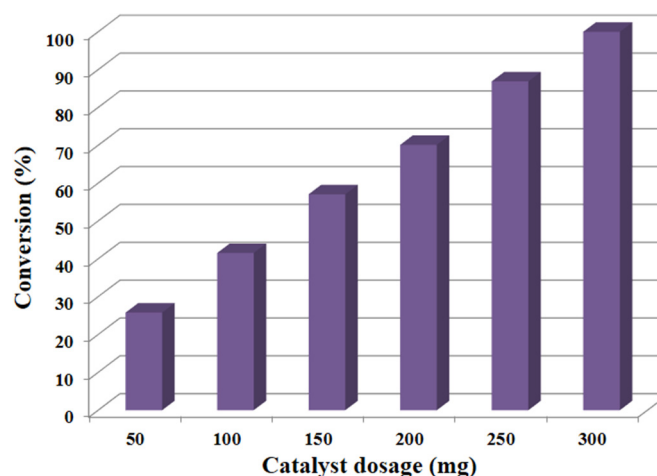
3.2.4. Influence of Dosage of Catalyst

To determine the optimal catalyst quantity, the oxidation of BzOH was carried out using different quantities of (1%)Co_xO_y-MnCO₃ catalyst, while other reaction conditions were kept constant, as optimized earlier, and the results are summarized in Table 4 and plotted in Figure 8. The results indicated that conversion of BzOH increases with raising catalyst quantity, while BzH selectivity was found to be same (>99%). When the catalyst quantity was raised from 50 to 300 mg, BzOH conversion to BzH was found to improve from 25.7% to 100% within 20 min (Entries 1–6). The current study reveals that just 0.3 g of catalyst is needed for accomplishing entire conversion of BzOH to BzH in a relatively short time interval.

Table 4. Catalyst quantity optimization.

Entry	Quantity (mg)	Conversion (%)	Specific Activity (mmol/g·h)	Selectivity (%)
1	50	25.8	30.9	>99
2	100	41.6	24.9	>99
3	150	57.1	22.8	>99
4	200	70.1	21.0	>99
5	250	86.9	20.8	>99
6	300	100.0	20.0	>99

Conditions: catalyst (1%)Co_xO_y-MnCO₃ calcined at 300 °C, 2 mmol BzOH, 15 mL toluene, 25 mL/min O₂ rate, 100 °C, 20 min.

**Figure 8.** Conversion of BzOH as a function of catalyst (1%)Co_xO_y-MnCO₃ dosage.

To ascertain the necessity of the catalyst presence for completion of this process, the blank oxidation reaction (without catalyst) was performed at optimum conditions. The result demonstrated that the reaction was not initiated, i.e. no BzH is detected, which proves the importance of the catalyst in this oxidation transformation. Similarly, a blank reaction was carried out in the absence of the reactant (BzOH) using (1%)Co_xO_y-MnCO₃ catalyst in presence of the solvent (toluene) to confirm that the solvent used in this experiment was not undergoing oxidation instead of the intended BzOH oxidation. As expected, traces of BzH were observed, implying that the desired BzH was only produced due to

catalytic oxidation of BzOH and not from oxidation of the solvent. Further, another study was carried out to elucidate the importance of oxygen molecule as sole oxidant. The oxidation experiment was performed using (1%)Co_xO_y-MnCO₃ catalyst in the absence of the bubbling O₂. The results revealed only 28.6% conversion, which is considerably lower than 100% conversion achieved when the process was conducted using O₂ molecule as an oxidizing agent.

A reasonable mechanism can only be suggested by using in-situ spectroscopic approaches. Nevertheless, according to reported publications in the catalysis field, the dehydrogenation step usually acts as rate-determining step in catalytic oxidation of alcohols [43]. Furthermore, the existence of a promoter (base or catalyst support) can assist to activate the O-H bond existent in alcohols to accelerate the oxidation rate. Herein, in the present catalytic protocol, Co_xO_y deposited on MnCO₃ was acting as promoter (basic sites Co_xO_y) [44]. In the presence of gaseous O₂, manganese in the MnCO₃ readily oxidized to high valence Mn, most probably to γ -MnOOH [45], and BzOH oxidized at the expense of these high valence Mn active sites. According to Tang and his group [46] and confirmed by others, we also suppose that this mechanism obeys the Marvan-Krevenlen oxidation mechanism. The active species is probably O²⁻ and most probable includes the transfer of two electrons in a single step. As the mechanism includes the interchange of O₂ from lattices, the catalytic performance is highly depended on Mn-O bond strength in Mn-based catalysts. This is probably due to the fact that Co_xO_y-MnCO₃ has higher activity where the surface Mn is oxidized to γ -MnOOH by gaseous O₂ and behaves more as a catalytic site than Co_xO_y-Mn₂O₃.

3.3. Recovery Tests

The recyclability of catalysts is an extremely important topic for cost reduction in industrial applications, therefore the repeatability of (1%)Co_xO_y-MnCO₃ for the aerial oxidation of BzOH was assessed under optimum circumstances and the attained data is depicted in Figure 9. The recovery data disclosed that the prepared catalyst is capable of reuse for six runs without noticeable loss in its activity after each run. The BzOH conversion product declined slightly from 100% to 91.1% after six subsequent cycles, which can be ascribed to trivial weight loss of the catalyst during the washing and filtration process [11]. Interestingly, the selectivity to BzH was intact (>99) during all recyclability tests. These observations indicate that the prepared catalyst is resistant to deactivation in catalytic oxidation of BzOH.

Moreover, to demonstrate the outstanding catalytic efficiency of our catalytic protocol, the performance of our catalyst was compared with other cobalt-possessing catalysts found in the previous publications and the findings are summarized in Table 5. The data revealed that, among all mentioned catalysts, the (1%)Co_xO_y-MnCO₃ catalyst seems to be the most efficacious catalyst for oxidation of BzOH in terms of conversion, specific activity, and reaction time. The present catalyst i.e., (1%)Co_xO_y-MnCO₃, achieved 100% BzOH conversion as well as >99 BzH selectivity within a relatively short period of 20 min at 100 °C as well as the highest specific activity (20 mmol/g-h) when compared to listed catalysts. Notably, other reported cobalt-based catalysts required a much longer time or higher temperature to achieve 100% conversion of BzOH. In this context, Jha and his co-workers [47] have synthesized the manganese and cobalt oxides incorporated on reduced graphene oxide (MnCoO-(1%)RGO) nanocomposites via the solvothermal procedure and employed these as an oxidative catalyst for BzOH oxidation. MnCoO-(1%)RGO nanocomposite gave about 78% BzOH conversion and 100% selectivity to BzH along with lower specific activity (12.6 mmol/g-h) after 2 h, which is a longer reaction time relative to that required by our catalyst. In another example, Ragupathi and co-workers [48] reported the use of cobalt aluminate nanoparticles (CoAl₂O₄) as a heterogeneous catalyst utilizing H₂O₂ as an oxidizing agent for oxidation of BzOH, but it required a much longer period of 8 h to give 96% alcohol conversion as well as having lower specific activity (1.2 mmol/g-h) when compared with our catalytic system. However, when the catalyst (1%)Co_xO_y-MnCO₃ was compared with various other Mn-based catalysts it was found that the present catalyst was better, with specific activity 20 mmol/g-h, than ZrO_x(1%)-MnCO₃, ZnO_x(1%)-MnCO₃,

or $\text{Ag}_2\text{O}(1\%)\text{-MnO}_2$, which showed specific activity of 13.3 mmol/g·h, 16.0 mmol/g·h, and 3.3 mmol/g·h, respectively. However, their graphene-based nanocomposites were found to be much better than the present catalyst.

The probable mechanism of the oxidation process by the Mars–van-Krevelen mechanism is depicted in Figure 10.

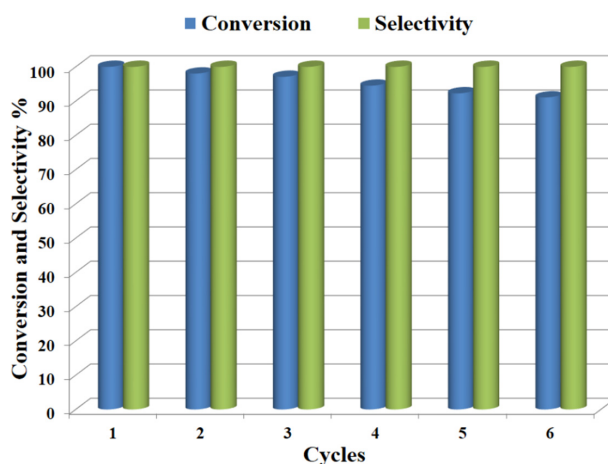


Figure 9. Stability and recyclability study of $(1\%)\text{Co}_x\text{O}_y\text{-MnCO}_3$ catalyst in oxidation of BzOH, Conditions: 0.3 g $(1\%)\text{Co}_x\text{O}_y\text{-MnCO}_3$ catalyst calcined at 300 °C, 2 mmol BzOH, 15 mL toluene, 25 mL/min O_2 rate, 100 °C, 20 min.

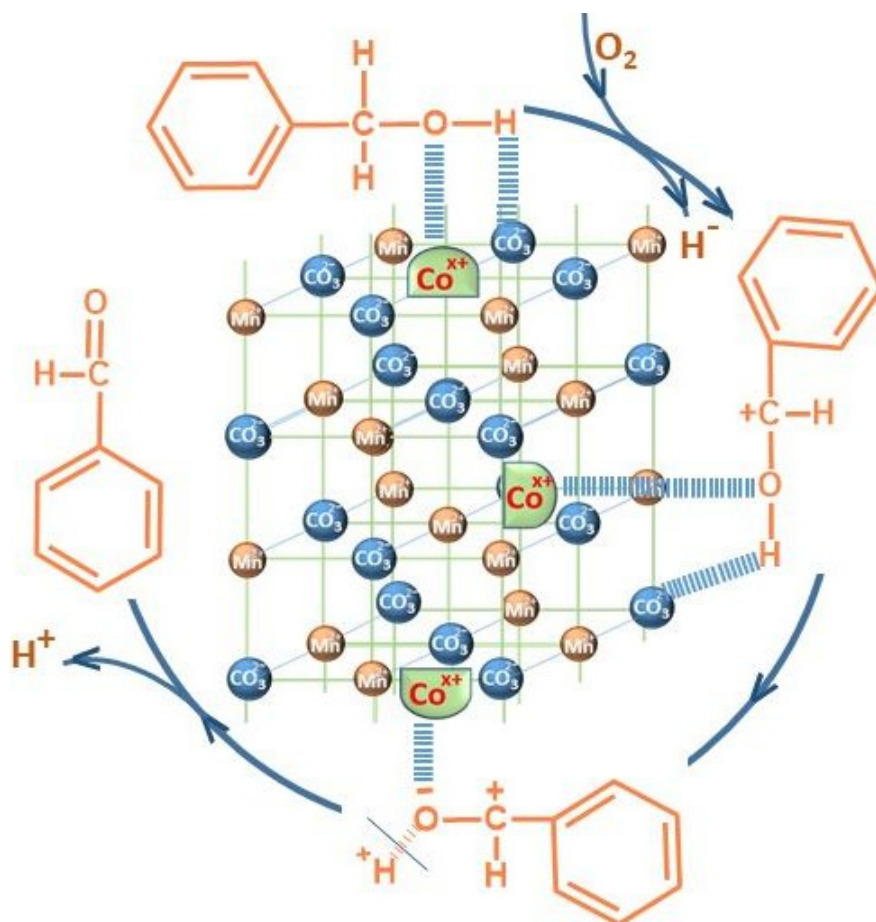


Figure 10. A plausible mechanism detailing the reaction pathway for oxidation of benzyl alcohol to benzaldehyde on the $(1\%)\text{Co}_x\text{O}_y\text{-MnCO}_3$ surface.

Table 5. Comparison of the effectiveness our catalyst and previously-reported cobalt-containing catalysts.

	Catalyst	Conversion (%)	Selectivity (%)	Time (h)	Temperature (°C)	Specific Activity (mmol/g·h)	Ref.
1.	(1%)Co _x O _y -MnCO ₃	100.0	>99	0.3	100	20.0	Herein
2.	MnCoO-(1%)RGO	78.0	100.0	2	140	12.6	[47]
3.	ZrO _x (1%)-MnCO ₃	100.0	>99	0.5	100	13.3	[49]
4.	Ag ₂ O(1%)-MnO ₂	100.0	>99	2.0	100	3.3	[50]
5.	ZnO _x (1%)-MnCO ₃	100.0	>99	0.42	100	16.0	[51]
6.	ZrO _x (1%)-MnCO ₃ /(1%)HRG	100.0	>99	0.15	100	44.4	[32]
7.	Ag ₂ O(1%)-MnO ₂ /(5%)HRG	100.0	>99	0.58	100	11.4	[34]
8.	ZnO _x (1%)-MnCO ₃ /(1%)HRG	100.0	>99	0.12	100	57.1	[33]
9.	CoAl ₂ O ₄	96.0	98.9	8	80	1.2	[48]
10.	Co/NG	89.5	97.3	8	100	4.5	[52]
11.	Co ₃ O ₄ -SBA-15	31.0	73.0	12	reflux	5.2	[31]
12.	CoO _x /RGO-HP	96.0	>99	6	110	14.8	[53]
13.	Co/Al ₂ O ₃	93.0	-	1	reflux	18.6	[4]
14.	VPO-Co	66.0	74.0	8	90	8.3	[54]
15.	CoPc/PANI	82.0	-	4	65	2.1	[55]
16.	Co ₃ O ₄ /MnO ₂	93.0	99.0	6	100	6.2	[28]
17.	[Co(bpy) ₂] ²⁺	53.0	100.0	8	reflux	4.0	[56]
18.	PMO ₁₁ Co	56.5	90.9	24	90	11.8	[57]
19.	Ru-Co-Ce	92.3	100	6	60	12.3	[58]

3.4. General Applicability of (1%)Co_xO_y-MnCO₃ Catalyst

After optimization of the reaction conditions, these were extended to several types of alcohols (e.g., aromatic, aliphatic, heterocyclic, and allylic alcohols) to show the versatility of (1%)Co_xO_y-MnCO₃ catalyst. The obtained catalytic data are outlined in Table 6. Interestingly, all primary aromatic alcohols were easily oxidized into their respective aldehydes with 100% conversions within short times using the above-optimized reaction conditions without any detectable overoxidation to acids (Entries 1–19). In addition, superior selectivity to respective aldehydes or ketones (more than 99%) was achieved for any case of alcohol in the present study and no by-products were noticed. The electronic nature of substituents on the benzylic alcohols exhibited a considerable impact on the catalytic performance depending on their ability to donate electrons to the aromatic ring [47]. It was found that aromatic alcohols possessing electron-releasing substituents were more favorable to the formation of their corresponding aldehydes than electron-withdrawing groups. In this regard, the benzyl alcohol possessing an electron-donating group (e.g., 4-methylbenzyl alcohol), was wholly oxidized to 4-methylbenzaldehyde within 25 min (Entry 3), while, 4-nitrobenzyl alcohol, that bears an electron-withdrawing group, needed a relatively-longer reaction time (45 min) (Entry 12). It was also clearly noticed that the p-substituted aromatic alcohols were completely transformed within relatively shorter reaction times by comparing with the o- and m- positions, possibly because the p-position has less steric hindrance with respect to the other positions [59]. p-Nitrobenzyl alcohol exhibited 100% conversion within only 45 min (Entry 12), whereas m- and o-nitrobenzyl alcohol were fully transformed after a longer time of 55 and 70 min, respectively (Entries 14 and 16). Also, steric resistance had an explicit impact on the oxidation rate; the bulky substituents (e.g., dichloro, trifluoromethyl, trimethoxy, and pentafluoro) connected to aromatic rings decreased the effectiveness of the catalytic system. This was due to steric hindrance that hindered the oxidation of aromatic alcohols possessing bulky groups (Entries 15,17–19). Heterocyclic alcohols, like furfuryl alcohol, were selectively oxidized to furfural after short time of 95 min (Entry 20). Additionally, allylic alcohols such cinnamyl alcohol were also efficiently converted to cinnamaldehyde with 100% conversion as well as selectivity within 30 min (Entry 21). With respect to the typical secondary aromatic alcohols, complete conversion and selectivity towards corresponding ketones was accomplished (Entries 22–27).

Indeed, compared to aromatic alcohols, the oxidation of aliphatic counterparts is much more complicated under the same circumstances [60]. However, our catalytic strategy was also found to be efficacious for oxidation of primary aliphatic alcohols. In this context, the oxidation of 5-hexenol, octanol, and citronellol to respective aldehydes occurred over slightly longer periods (Entries 29–31). With respect to secondary aromatic alcohols, the oxidation of secondary aliphatic alcohols into respective ketones showed a relatively lower performance towards this transformation (Entries 32–34). Apparently, it was necessary to increase the time of the reaction, owing to the fact that oxidation of aromatic alcohols is easier than that of their aliphatic counterparts. As predicted, entire oxidation of 1-phenyl-ethanol took place after just 35 min, whereas the total oxidation of 2-octanol took place within a longer time of 250 min (Entries 24 and 34), which confirms that, the as-prepared catalyst's performance was impacted by electronic and steric variables.

Table 6. (1%)Co_xO_y-MnCO₃-catalyzed oxidation of different kinds of alcohols employing gaseous O₂ under free-alkali circumstances.

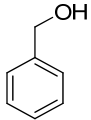
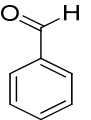
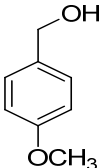
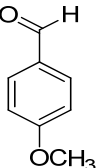
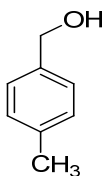
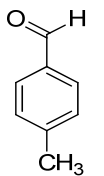
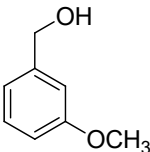
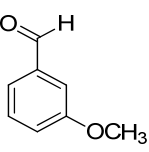
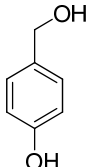
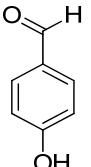
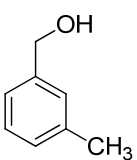
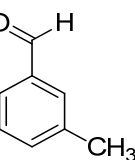
Entry	Alcohols	Carbonyls	Time (minutes)	Conversion (%) –Selectivity (%)
1			20	100 – >99
2			25	100 – >99
3			25	100 – >99
4			30	100 – >99
5			30	100 – >99
6			35	100 – >99

Table 6. Cont.

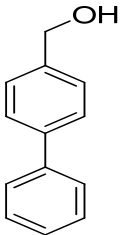
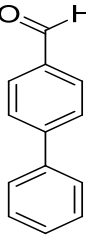
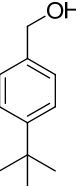
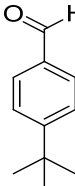
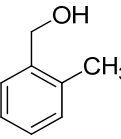
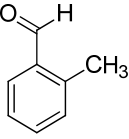
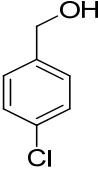
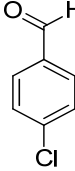
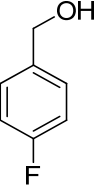
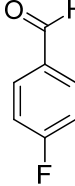
Entry	Alcohols	Carbonyls	Time (minutes)	Conversion (%) –Selectivity (%)
7			35	100 – >99
8			35	100 – >99
9			40	100 – >99
10			40	100 – >99
11			45	100 – >99

Table 6. Cont.

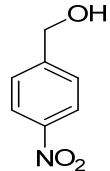
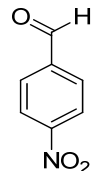
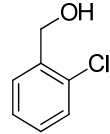
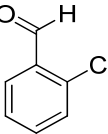
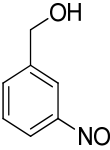
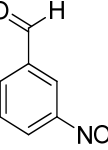
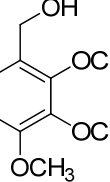
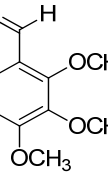
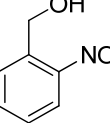
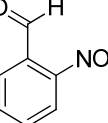
Entry	Alcohols	Carbonyls	Time (minutes)	Conversion (%) –Selectivity (%)
12			45	100 – >99
13			50	100 – >99
14			55	100 – >99
15			65	100 – >99
16			70	100 – >99

Table 6. Cont.

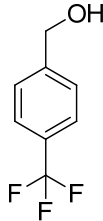
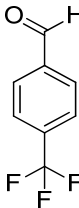
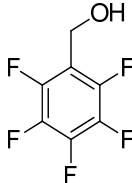
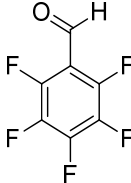
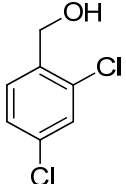
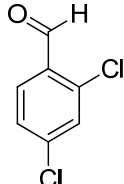
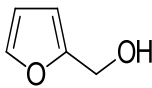
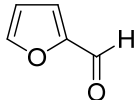
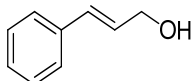
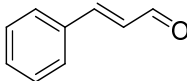
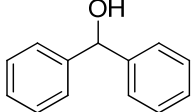
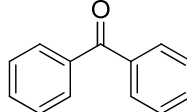
Entry	Alcohols	Carbonyls	Time (minutes)	Conversion (%) –Selectivity (%)
17			70	100 – >99
18			70	100 – >99
19			75	100 – >99
20			95	100 – >99
21			30	100 – >99
22			35	100 – >99

Table 6. Cont.

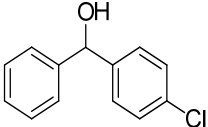
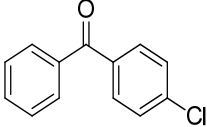
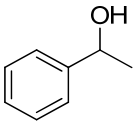
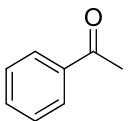
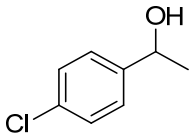
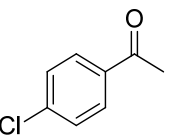
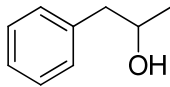
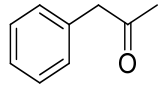
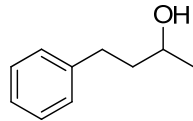
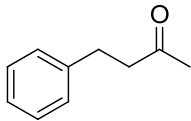
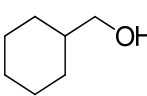
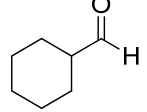
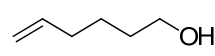
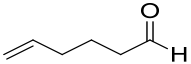
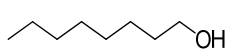
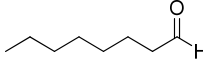
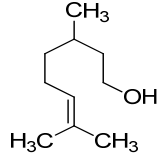
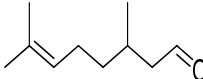
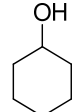
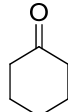
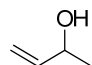
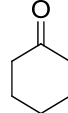
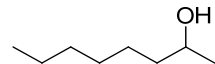
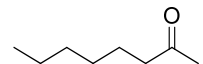
Entry	Alcohols	Carbonyls	Time (minutes)	Conversion (%) –Selectivity (%)
23			45	100 – >99
24			35	100 – >99
25			40	100 – >99
26			35	100 – >99
27			45	100 – >99
28			75	100 – >99
29			190	100 – >99
30			240	100 – >99

Table 6. Cont.

Entry	Alcohols	Carbonyls	Time (minutes)	Conversion (%) –Selectivity (%)
31			130	100 – >99
32			90	100 – >99
33			230	100 – >99
34			250	100 – >99

Conditions: 2 mmol substrate, 0.3 g (1%)Co_xO_y–MnCO₃ catalyst calcined at 300 °C, 15 mL toluene, 25 mL/min O₂ rate, 100 °C.

4. Conclusions

A comparative catalytic assessment of Co_xO_y -doped MnCO_3 [(1%) Co_xO_y - MnCO_3] and Co_xO_y -doped Mn_2O_3 [(1%) Co_xO_y - Mn_2O_3] synthesized through a co-precipitation procedure was carried out. It was found that the catalyst (1%) Co_xO_y - MnCO_3 exhibited superior effectiveness when compared to its oxide counterpart i.e., (1%) Co_xO_y - Mn_2O_3 . Amongst the different catalysts synthesized by varying the weight percentage of Co_xO_y supported on MnCO_3 , (1%) Co_xO_y - MnCO_3 demonstrates excellent catalytic efficiency in aerial oxidation of BzOH employing gaseous O_2 . Notably, the catalytic activity was considerably enhanced after incorporating Co_xO_y on MnCO_3 in this oxidation transformation. A complete conversion of BzOH with >99% selectivity to BzH was achieved in only 20 min alongside specific activity of 20 mmol/g·h, which is considerably higher than that obtained for several cobalt-containing catalysts in former publications for this transformation. In addition, aerial oxidation of a wide range of aromatic, aliphatic, secondary, heterocyclic, and allylic alcohols to their respective ketones or aldehydes was also tested. These gave full convertibility within short times without yielding any further oxidation product. The attained results suggested that our catalysts are highly selective towards the aromatic alcohols. Additionally, (1%) Co_xO_y - MnCO_3 can be efficiently regenerated six consecutive times with no discernible loss in its efficiency and selectivity and it stayed roughly intact. This catalytic system possesses several features including being a simple and straightforward procedure, utilizing a clean oxidizing agent, having full convertibility and selectivity, requiring no addition of surfactants or bases, having wide substrate applicability, and being a rapid reaction with mild circumstances, facile recovery, and stable catalyst.

Supplementary Materials: The following are available online at <http://www.mdpi.com/2227-9717/8/8/910/s1>, Figure S1: EDS analysis of synthesized catalysts (a) (1%) Co_3O_4 - MnCO_3 and (b) (1%) Co_3O_4 - Mn_2O_3 .

Author Contributions: S.F.A. and O.A. designed the project; M.E.A., M.K. (Mujeeb Khan), and M.R.S. helped to draft the manuscript; K.M.M., D.S. and M.K. (Mufsir Kuniyil) carried out the experimental part and some parts of the characterization; A.K., A.Z.D., and M.K. (Mufsir Kuniyil) carried out some parts of the characterization. A.A.-W. and M.R.H.S. provided scientific guidance for successful completion of the project and helped to draft the manuscript. All authors read and approved the final manuscript.

Funding: This work is funded by the research group project No. RG-1440-068.

Acknowledgments: The authors extend their appreciation to the Deanship of Scientific Research at King Saud University for funding this work through the research group project No. RG-1440-068.

Conflicts of Interest: The authors declare no conflict of interest.

References

1. Sheldon, R.A.; Arends, I.; Dijkstra, A. New developments in catalytic alcohol oxidations for fine chemicals synthesis. *Catal. Today* **2000**, *57*, 157–166. [CrossRef]
2. Adam, F.; Ooi, W.T. Selective oxidation of benzyl alcohol to benzaldehyde over Co-metalloporphyrin supported on silica nanoparticles. *Appl. Catal. A Gen.* **2012**, *445*, 252–260. [CrossRef]
3. Kamimura, A.; Nozaki, Y.; Ishikawa, S.; Inoue, R.; Nakayama, M. K-birnessite MnO_2 : A new selective oxidant for benzylic and allylic alcohols. *Tetrahedron Lett.* **2011**, *52*, 538–540. [CrossRef]
4. Albadi, J.; Alihosseinzadeh, A.; Jalali, M.; Shahrezaei, M.; Mansournezhad, A. Highly dispersed cobalt nanoparticles supported on a mesoporous Al_2O_3 : An efficient and recyclable catalyst for aerobic oxidation of alcohols in aqueous media. *Mol. Catal.* **2017**, *440*, 133–139. [CrossRef]
5. Shi, Z.; Zhang, C.; Tang, C.; Jiao, N. Recent advances in transition-metal catalyzed reactions using molecular oxygen as the oxidant. *Chem. Soc. Rev.* **2012**, *41*, 3381–3430. [CrossRef]
6. Sun, C.; Yang, J.; Dai, Z.; Wang, X.; Zhang, Y.; Li, L.; Chen, P.; Huang, W.; Dong, X. Nanowires assembled from MnCo_2O_4 @C nanoparticles for water splitting and all-solid-state supercapacitor. *Nano Res.* **2016**, *9*, 1300–1309. [CrossRef]
7. Zhou, C.; Guo, Z.; Dai, Y.; Jia, X.; Yu, H.; Yang, Y. Promoting role of bismuth on carbon nanotube supported platinum catalysts in aqueous phase aerobic oxidation of benzyl alcohol. *Appl. Catal. B Environ.* **2016**, *181*, 118–126. [CrossRef]

8. Zhu, J.; Figueiredo, J.L.; Faria, J.L. Au/activated-carbon catalysts for selective oxidation of alcohols with molecular oxygen under atmospheric pressure: Role of basicity. *Catal. Commun.* **2008**, *9*, 2395–2397. [[CrossRef](#)]
9. Wusiman, A.; Lu, C.D. Selective oxidation of benzylic, allylic and propargylic alcohols using dirhodium (II) tetraamidinate as catalyst and aqueous tert-butyl hydroperoxide as oxidant. *Appl. Organomet. Chem.* **2015**, *29*, 254–258. [[CrossRef](#)]
10. Yamaguchi, K.; Mizuno, N. Supported ruthenium catalyst for the heterogeneous oxidation of alcohols with molecular oxygen. *Angew. Chem. Int. Ed.* **2002**, *41*, 4538–4542. [[CrossRef](#)]
11. Li, M.; Wu, S.; Yang, X.; Hu, J.; Peng, L.; Bai, L.; Huo, Q.; Guan, J. Highly efficient single atom cobalt catalyst for selective oxidation of alcohols. *Appl. Catal. A* **2017**, *543*, 61–66. [[CrossRef](#)]
12. Cruz, P.; Pérez, Y.; del Hierro, I.; Fajardo, M. Copper, Copper Oxide Nanoparticles and Copper Complexes Supported on Mesoporous SBA-15 as Catalysts in the Selective Oxidation of Benzyl Alcohol in Aqueous Phase. *Microporous Mesoporous Mater.* **2016**, *220*, 136–147. [[CrossRef](#)]
13. Hajipour, A.R.; Karimi, H.; Koochi, A. Selective oxidation of alcohols over nickel zirconium phosphate. *Chin. J. Catal.* **2015**, *36*, 1109–1116. [[CrossRef](#)]
14. Cang, R.; Lu, B.; Li, X.; Niu, R.; Zhao, J.; Cai, Q. Iron-Chloride Ionic Liquid Immobilized on SBA-15 for Solvent-Free Oxidation of Benzyl Alcohol to Benzaldehyde with H₂O₂. *Chem. Eng. Sci.* **2015**, *137*, 268–275. [[CrossRef](#)]
15. Jiang, N.; Ragauskas, A.J. Vanadium-catalyzed selective aerobic alcohol oxidation in ionic liquid [bmim] PF₆. *Tetrahedron Lett.* **2007**, *48*, 273–276. [[CrossRef](#)]
16. Öztürk, Ö.F.; Zümreoğlu-Karan, B.; Karabulut, S. Solvent-free oxidation of benzyl alcohol over chromium orthoborate. *Catal. Commun.* **2008**, *9*, 1644–1648. [[CrossRef](#)]
17. Biradar, A.V.; Dongare, M.K.; Umbarkar, S.B. Selective oxidation of aromatic primary alcohols to aldehydes using molybdenum acetylido-oxo-peroxo complex as catalyst. *Tetrahedron Lett.* **2009**, *50*, 2885–2888. [[CrossRef](#)]
18. Goh, T.W.; Xiao, C.; Maligal-Ganesh, R.V.; Li, X.; Huang, W. Utilizing Mixed-Linker Zirconium Based Metal-Organic Frameworks to Enhance the Visible Light Photocatalytic Oxidation of Alcohol. *Chem. Eng. Sci.* **2015**, *124*, 45–51. [[CrossRef](#)]
19. Forouzani, M.; Mardani, H.R.; Ziari, M.; Malekzadeh, A.; Biparva, P. Comparative Study of Oxidation of Benzyl Alcohol: Influence of Cu-Doped Metal Cation on Nano ZnO Catalytic Activity. *Chem. Eng. J.* **2015**, *275*, 220–226. [[CrossRef](#)]
20. Ndolomingo, M.J.; Meijboom, R. Selective liquid phase oxidation of benzyl alcohol to benzaldehyde by tert-butyl hydroperoxide over γ -Al₂O₃ supported copper and gold nanoparticles. *Appl. Surf. Sci.* **2017**, *398*, 19–32. [[CrossRef](#)]
21. Guo, X.; Li, J.; Zhou, R. Catalytic performance of manganese doped CuO–CeO₂ catalysts for selective oxidation of CO in hydrogen-rich gas. *Fuel* **2016**, *163*, 56–64. [[CrossRef](#)]
22. Clarke, T.J.; Kondrat, S.A.; Taylor, S.H. Total Oxidation of Naphthalene Using Copper Manganese Oxide Catalysts. *Catal. Today* **2015**, *258 Pt 2*, 610–615. [[CrossRef](#)]
23. Kim, S.C.; Park, Y.-K.; Nah, J.W. Property of a highly active bimetallic catalyst based on a supported manganese oxide for the complete oxidation of toluene. *Powder Technol.* **2014**, *266*, 292–298. [[CrossRef](#)]
24. Feng, Z.; Xie, Y.; Hao, F.; Liu, P.; Luo, H.a. Catalytic oxidation of cyclohexane to KA oil by zinc oxide supported manganese 5, 10, 15, 20-tetrakis (4-nitrophenyl) porphyrin. *J. Mol. Catal. A Chem.* **2015**, *410*, 221–225. [[CrossRef](#)]
25. Piumetti, M.; Fino, D.; Russo, N. Mesoporous manganese oxides prepared by solution combustion synthesis as catalysts for the total oxidation of VOCs. *Appl. Catal. B Environ.* **2015**, *163*, 277–287. [[CrossRef](#)]
26. Burange, A.S.; Kale, S.R.; Jayaram, R.V. Oxidation of alkyl aromatics to ketones by tert-butyl hydroperoxide on manganese dioxide catalyst. *Tetrahedron Lett.* **2012**, *53*, 2989–2992. [[CrossRef](#)]
27. Pei, J.; Han, X.; Lu, Y. Performance and kinetics of catalytic oxidation of formaldehyde over copper manganese oxide catalyst. *Build. Environ.* **2015**, *84*, 134–141. [[CrossRef](#)]
28. Reddy, V.G.; Jampaiah, D.; Chalkidis, A.; Sabri, Y.M.; Mayes, E.L.; Bhargava, S.K. Highly dispersed cobalt oxide nanoparticles on manganese oxide nanotubes for aerobic oxidation of benzyl alcohol. *Catal. Commun.* **2019**, *130*, 105763. [[CrossRef](#)]
29. Li, M.; Fu, X.; Peng, L.; Bai, L.; Wu, S.; Kan, Q.; Guan, J. Synthesis of Three-Dimensional-Ordered Mesoporous Cobalt Oxides for Selective Oxidation of Benzyl Alcohol. *ChemSelect* **2017**, *2*, 9486–9489. [[CrossRef](#)]

30. Zhu, J.; Kailasam, K.; Fischer, A.; Thomas, A. Supported cobalt oxide nanoparticles as catalyst for aerobic oxidation of alcohols in liquid phase. *ACS Catal.* **2011**, *1*, 342–347. [[CrossRef](#)]
31. Taghavimoghaddam, J.; Knowles, G.P.; Chaffee, A.L. Mesoporous Silica SBA-15 Supported Co_3O_4 Nanorods as Efficient Liquid Phase Oxidative Catalysts. *Top. Catal.* **2012**, *55*, 571–579. [[CrossRef](#)]
32. Assal, M.E.; Shaik, M.R.; Kuniyil, M.; Khan, M.; Al-Warthan, A.; Siddiqui, M.R.H.; Khan, S.M.; Tremel, W.; Tahir, M.N.; Adil, S.F. A highly reduced graphene oxide/ $\text{ZrO}_x\text{-MnCO}_3$ or- Mn_2O_3 nanocomposite as an efficient catalyst for selective aerial oxidation of benzylic alcohols. *RSC Adv.* **2017**, *7*, 55336–55349. [[CrossRef](#)]
33. Assal, M.E.; Shaik, M.R.; Kuniyil, M.; Khan, M.; Alzahrani, A.Y.; Al-Warthan, A.; Siddiqui, M.R.H.; Adil, S.F. Mixed Zinc/Manganese on Highly Reduced Graphene Oxide: A Highly Active Nanocomposite Catalyst for Aerial Oxidation of Benzylic Alcohols. *Catalysts* **2017**, *7*, 391. [[CrossRef](#)]
34. Assal, M.E.; Shaik, M.R.; Kuniyil, M.; Khan, M.; Al-Warthan, A.; Alharthi, A.I.; Varala, R.; Siddiqui, M.R.H.; Adil, S.F. Ag_2O nanoparticles/ $\text{MnCO}_3\text{-MnO}_2$ or- Mn_2O_3 /highly reduced graphene oxide composites as an efficient and recyclable oxidation catalyst. *Arab. J. Chem.* **2019**, *12*, 54–68. [[CrossRef](#)]
35. Gac, W. The influence of silver on the structural, redox and catalytic properties of the cryptomelane-type manganese oxides in the low-temperature CO oxidation reaction. *Appl. Catal. B Environ.* **2007**, *75*, 107–117. [[CrossRef](#)]
36. Hu, H.; Xu, J.-y.; Yang, H.; Liang, J.; Yang, S.; Wu, H. Morphology-Controlled Hydrothermal Synthesis of MnCO_3 Hierarchical Superstructures with Schiff Base as Stabilizer. *Mater. Res. Bull.* **2011**, *46*, 1908–1915. [[CrossRef](#)]
37. Maslen, E.; Streltsov, V.; Streltsova, N.; Ishizawa, N. Electron density and optical anisotropy in rhombohedral carbonates. III. Synchrotron X-ray studies of CaCO_3 , MgCO_3 and MnCO_3 . *Acta Crystallogr. Sect. B Struct. Sci.* **1995**, *51*, 929–939. [[CrossRef](#)]
38. Dubal, D.; Dhawale, D.; Salunkhe, R.; Pawar, S.; Lokhande, C. A novel chemical synthesis and characterization of Mn_3O_4 thin films for supercapacitor application. *Appl. Surf. Sci.* **2010**, *256*, 4411–4416. [[CrossRef](#)]
39. Zhu, C.; Saito, G.; Akiyama, T. A new CaCO_3 -template method to synthesize nanoporous manganese oxide hollow structures and their transformation to high-performance LiMn_2O_4 cathodes for lithium-ion batteries. *J. Mater. Chem. A* **2013**, *1*, 7077–7082. [[CrossRef](#)]
40. Sreethawong, T.; Ngamsinlapasathian, S.; Yoshikawa, S. Facile surfactant-aided sol-gel synthesis of mesoporous-assembled Ta_2O_5 nanoparticles with enhanced photocatalytic H_2 production. *J. Mol. Catal. A Chem.* **2013**, *374*, 94–101. [[CrossRef](#)]
41. Smoláková, L.; Kout, M.; Koudelková, E.; Čapek, L. Effect of Calcination Temperature on the Structure and Catalytic Performance of the $\text{Ni}/\text{Al}_2\text{O}_3$ and $\text{Ni-Ce}/\text{Al}_2\text{O}_3$ Catalysts in Oxidative Dehydrogenation of Ethane. *Ind. Eng. Chem. Res.* **2015**, *54*, 12730–12740. [[CrossRef](#)]
42. Kunkalekar, R.; Salker, A. Low temperature carbon monoxide oxidation over nanosized silver doped manganese dioxide catalysts. *Catal. Commun.* **2010**, *12*, 193–196. [[CrossRef](#)]
43. Su, F.Z.; Liu, Y.M.; Wang, L.C.; Cao, Y.; He, H.Y.; Fan, K.N. Ga-Al Mixed-Oxide-Supported Gold Nanoparticles with Enhanced Activity for Aerobic Alcohol Oxidation. *Angew. Chem. Int. Ed.* **2008**, *120*, 340–343. [[CrossRef](#)]
44. Ishida, T.; Takamura, R.; Takei, T.; Akita, T.; Haruta, M. Support effects of metal oxides on gold-catalyzed one-pot N-alkylation of amine with alcohol. *Appl. Catal. A* **2012**, *413*, 261–266. [[CrossRef](#)]
45. Jun, Y.-S.; Kendall, T.A.; Martin, S.T.; Friend, C.M.; Vlassak, J.J. Heteroepitaxial nucleation and oriented growth of manganese oxide islands on carbonate minerals under aqueous conditions. *Environ. Sci. Technol.* **2005**, *39*, 1239–1249. [[CrossRef](#)]
46. Tang, Q.; Gong, X.; Wu, C.; Chen, Y.; Borgna, A.; Yang, Y. Insights into the nature of alumina-supported MnOOH and its catalytic performance in the aerobic oxidation of benzyl alcohol. *Catal. Commun.* **2009**, *10*, 1122–1126. [[CrossRef](#)]
47. Jha, A.; Mhamane, D.; Suryawanshi, A.; Joshi, S.M.; Shaikh, P.; Biradar, N.; Ogale, S.; Rode, C.V. Triple nanocomposites of CoMn_2O_4 , Co_3O_4 and reduced graphene oxide for oxidation of aromatic alcohols. *Catal. Sci. Technol.* **2014**, *4*, 1771–1778. [[CrossRef](#)]
48. Ragupathi, C.; Vijaya, J.J.; Narayanan, S.; Jesudoss, S.; Kennedy, L.J. Highly Selective Oxidation of Benzyl Alcohol to Benzaldehyde with Hydrogen Peroxide by Cobalt Aluminate Catalysis: A Comparison of Conventional and Microwave Methods. *Ceram. Int.* **2015**, *41*, 2069–2080. [[CrossRef](#)]

49. Assal, M.E.; Kuniyil, M.; Khan, M.; Al-Warthan, A.; Siddiqui, M.R.H.; Tremel, W.; Nawaz Tahir, M.; Adil, S.F. Synthesis and Comparative Catalytic Study of Zirconia–MnCO₃ or–Mn₂O₃ for the Oxidation of Benzylic Alcohols. *ChemOpen* **2016**, *6*, 112–120.
50. Assal, M.E.; Shaik, M.R.; Kuniyil, M.; Khan, M.; Venkata, S.J.; Alzahrani, A.Y.; Al-Warthan, A.; Al-Tamrah, S.A.; Siddiqui, M.R.H.; Hashmi, S.A.; et al. Silver-doped manganese based nanocomposites for aerial oxidation of alcohols. *Mater. Express* **2018**, *8*, 35–54. [[CrossRef](#)]
51. Adil, S.F.; Assal, M.E.; Kuniyil, M.; Khan, M.; Shaik, M.R.; Alwarthan, A.; Labis, J.P.; Siddiqui, M.R.H. Synthesis and Comparative Catalytic Study of Zinc Oxide (ZnO_x) Nanoparticles Promoted MnCO₃, MnO₂ and Mn₂O₃ for Selective Oxidation of Benzylic Alcohols Using Molecular Oxygen. *Mater. Express* **2017**, *7*, 79–92. [[CrossRef](#)]
52. Yang, X.; Wu, S.; Hu, J.; Fu, X.; Peng, L.; Kan, Q.; Huo, Q.; Guan, J. Highly efficient N-doped magnetic cobalt-graphene composite for selective oxidation of benzyl alcohol. *Catal. Commun.* **2016**, *87*, 90–93. [[CrossRef](#)]
53. Wu, Y.; Yu, H.; Wang, H.; Peng, F. Controllable synthesis and catalytic performance of graphene-supported metal oxide nanoparticles. *Chin. J. Catal.* **2014**, *35*, 952–959. [[CrossRef](#)]
54. Mahdavi, V.; Hasheminasab, H.R. Vanadium phosphorus oxide catalyst promoted by cobalt doping for mild oxidation of benzyl alcohol to benzaldehyde in the liquid phase. *Appl. Catal. A* **2014**, *482*, 189–197. [[CrossRef](#)]
55. Panwar, V.; Kumar, P.; Ray, S.S.; Jain, S.L. Organic inorganic hybrid cobalt phthalocyanine/polyaniline as efficient catalyst for aerobic oxidation of alcohols in liquid phase. *Tetrahedron Lett.* **2015**, *56*, 3948–3953. [[CrossRef](#)]
56. Peyrovi, M.; Mahdavi, V.; Salehi, M.; Mahmoodian, R. Oxidation of alcohols with tert-butylhydroperoxide catalyzed by Co (II) complexes immobilized between silicate layers of bentonite. *Catal. Commun.* **2005**, *6*, 476–479. [[CrossRef](#)]
57. Pathan, S.; Patel, A. Solvent free clean selective oxidation of alcohols catalyzed by mono transition metal (Co, Mn, Ni)-substituted Keggin-phosphomolybdates using hydrogen peroxide. *Appl. Catal. A* **2013**, *459*, 59–64. [[CrossRef](#)]
58. Liu, G.; Liu, J.; Li, W.; Liu, C.; Wang, F.; He, J.; Guild, C.; Jin, J.; Kriz, D.; Miao, R. Aerobic oxidation of alcohols over Ru-Mn-Ce and Ru-Co-Ce catalysts: The effect of calcination temperature. *Appl. Catal. A* **2017**, *535*, 77–84. [[CrossRef](#)]
59. Hosseini-Sarvari, M.; Ataee-Kachouei, T.; Moeini, F. A Novel and Active Catalyst Ag/ZnO for Oxidant-Free Dehydrogenation of Alcohols. *Mater. Res. Bull.* **2015**, *72*, 98–105. [[CrossRef](#)]
60. Xu, C.; Zhang, L.; An, Y.; Wang, X.; Xu, G.; Chen, Y.; Dai, L. Promotional synergistic effect of Sn doping into a novel bimetallic Sn-W oxides/graphene catalyst for selective oxidation of alcohols using aqueous H₂O₂ without additives. *Appl. Catal. A* **2018**, *558*, 26–33. [[CrossRef](#)]

